24th COBEM - 2017

24th ABCM International Congress of Mechanical Engineering
December 3-8, 2017, Curitiba, PR, Brazil

COBEM-2017-0571
BUILDING AND TESTING OF A LAB-SCALE HYBRID ROCKET MOTOR FOR ACQUISITION OF REGRESSION RATE EQUATIONS

Guilherme Engler
Thaís Maia Araújo
Federal University of ABC, Sao Bernardo do Campo, Brazil
aeroengler@gmail.com
maia.thais@ufabc.edu.br

Leonardo Henrique Gouvêa
National Institute For Space Research, Cachoeira Paulista, Brazil
samura.leo@gmail.com

Fernando de Souza Costa
National Institute For Space Research, Cachoeira Paulista, Brazil
fernando@lcp.inpe.br

Abstract. *A lab-scale hybrid rocket motor was designed, built and tested to develop a methodology to determine average fuel regression rate. Also, due to operational safety of hybrid rocket motors, propellants' low-cost acquisition and possibility to acquire a large amount of data per experiment, leading to more accurate results, the system was intended for learning purposes. The crystal solid fuel used was polymethyl methacrylate (PMMA) and the combustion processes were performed with axial oxidizer injection of gaseous oxygen (GOX). A modular apparatus was developed permitting adaptation for different test conditions and data acquisitions, i.e., operates as a motor or combustion chamber. Grain sizing analysis was conducted and the optimal initial port diameter and oxidizer mass flow rate were determined. The optical data acquisitions, performed by a high-speed camera, provided a large number of information that after being processed resulted in a regression rate expression of the fuel. Comparisons with data from the literature were carried out and the regression rate obtained in this work proved to be in complete agreement. In summary, the good regression rate results allied with the facts of safe operational condition and low-cost indicated that lab-scale hybrid rocket motors should be very appropriate for educational applications.*

Keywords: *propulsion, hybrid rocket, regression rate, PMMA.*

1. INTRODUCTION

Hybrid rocket motors are known for combining both solid and fluid propellants. According to Sutton and Biblarz (2010), they are of considerable interest due to their advantages such as enhanced safety from explosion or detonation during fabrication, storage and operation; start-stop-restart capabilities, and relative simplicity due to the necessity of only half the plumbing when compared, for example to liquid propellant systems.

The history of hybrid rockets motors dates back to the early 1930s, when Sergei P. Korolev and Mikhail K. Tikhonravov launched a 500 N motor using gasoline and collophonium, a gelled form of gasoline, and reached 1500 m. Later that decade, L. Andrussow, O. Lutz, and W. Noeggerath conducted tests on a 10 kN hybrid motor using coal and gaseous nitrous oxide, however without success. The earliest significant effort of a flightworthy hybrid rocket motor was conducted in the 1940s by the Pacific Rocket Society employing wood and rubber-based fuels, and liquid oxygen as oxidizer. After several attempts, it was possible to reach an altitude of 30,000 ft (Kuo and Chiaverini, 2007).

Hybrid propellant rockets have encountered a modern usage in sounding rockets (Zilliac *et al.*, 2012), launch boosters as those developed by the American Company Rocket, which could produce 110 kN of thrust (Kuo and Chiaverini, 2007). Additionally, hybrids are also present in small satellite propulsion systems such as the one applied by Simurda *et al.* (2013), that combined PMMA and nitrous oxide in an attempt to operate an inexpensive system with environmentally benign propellants. Furthermore, there is an increasing enthusiasm regarding suborbital space tourism, which creates an opportunity to the development of such form of propulsion (Frank *et al., 2014*).

Therefore, due to the wide variety of innovative applications, it became important to understand characteristics and phenomena associated to hybrid rocket motors in order to motivate aerospace engineering students to get in touch with the methodology and experimental procedures involving rockets. Other advantages offered by hybrid rocket motors are the safer operation when compared to solid and liquid propellants, and can be made with low-cost, which encourage their application for educational purposes. Thus, the present work proposed the development and construction of a lab scale hybrid rocket motor for acquisition of one of the most important parameters for hybrid rocket design and performance prediction, the fuel regression rate, that is the receding rate of the fuel along the burn interval. The conception of the apparatus was carefully focused in simplicity and functionality leading to a modular design which permitted alterations and adaptation for different tests conditions and distinct data acquisitions, for instance it would be possible to operate the apparatus as a motor or combustion chamber, i.e., with or without a nozzle, respectively. For this project, it was adopted a combustion chamber configuration, gaseous oxygen (GOX) was chosen as oxidizer and polymethyl methacrylate (PMMA) as fuel. The choice of PMMA as fuel was due to two of its characteristics: it is safely handled in ambient conditions, and its crystal characteristic that allows visual data acquisition for regression rate analysis. The construction and testing of the apparatus occurred in the Laboratory of Combustion and Propulsion associated to the National Institute for Space Research (LCP-INPE).

2. PRELIMINARY SIMULATIONS AND GRAIN SIZING

In this work, grain sizing was achieved through the studies of parameters such as the mixture ratio O/F that relates the quantities of fuel and oxidizer, the characteristic velocity (C^*) which is useful when comparing the relative performance of different chemical rocket propulsion system designs and propellants (Sutton and Biblarz, 2010), the oxidizer mass flow rate, $\dot{m}_{ox}$, and burn time, t_b.

Due to availability and low-cost reasons the external diameter and length of the grains were preset as 45 and 195 millimeters, respectively, while the internal diameter or port diameter was calculated, and resulted in 10 millimeters. The main dimensions of the final grain's geometry are illustrated in Fig. 1. In order to attain the 10 millimeters port diameter, simulations were conducted involving the relation between the characteristic velocity and the mixture ratio.

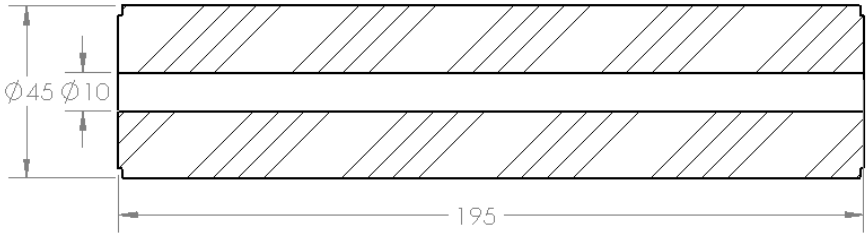

Figure 1. Geometry and dimensions in millimeters of the tested fuel grain.

Utilizing the free distribution software "Chemical Equilibrium with Applications – CEAgui-Nasa" (McBride and Gordon, 2002), it was possible to simulate the PMMA-O_2 burn reaction, applying mixture ratio ranging from O/F = 1 to O/F = 3. This range was defined to guarantee the inclusion of the stoichiometric mixture ratio value of O/F_{st} = 2. The analysis from the simulations provided data for the acquisition of characteristic velocity curves. The characteristic velocity variation curves with respect to the mixture ratio for four different values of pressure in the chamber are shown in Fig. 2. The pressure variations from 3 to 6 bar were chosen to avoid possible instabilities that occur when working under 3 bar, and also to explore the implications of relatively higher levels of pressure. Analyzing the curves, it was possible to notice that, regardless the pressure value in the chamber, the maximum characteristic velocity was attained for O/F = 1.2, which is approximately the typical value for operations with PMMA according to Marxman and Gilbert (1963).

After the optimum mixture ratio value was obtained, it was necessary to define the initial port diameter and the oxidizer mass flow rate. These parameters were achieved through an iterative process, that required the application of regression rate data suggested by Zilliac and Karabeyoglu (2006) as a first approach to the problem. In this work the oxidizer mass flow rate was set at a constant value throughout the experiments, for that matter the authors preset a burn time of sixty seconds.

There is an interdependence between the mixture ratio O/F and the average fuel regression rate ($\bar{r}$), i.e., once the oxidizer mass flow rate was set to be constant it was expected the decrease of the regression rate through the burn time, occasioning an increase of the mixture ratio value.

The initial port diameter and oxidizer mass flow rate were determined as 10 millimeters and 0.5g/s, respectively, and these values were validated by obtaining the curve illustrated in Fig. 3, demonstrating that for 30 seconds, half of the burn time, the O/F is around 1.2.

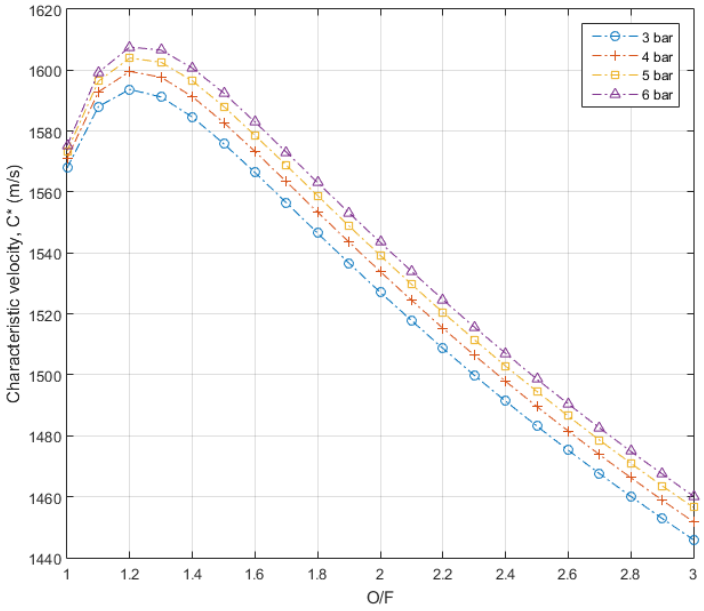

Figure 2. Variation of the characteristic velocity, C^* for an O/F interval from 1 to 3, for four pressure values in the chamber.

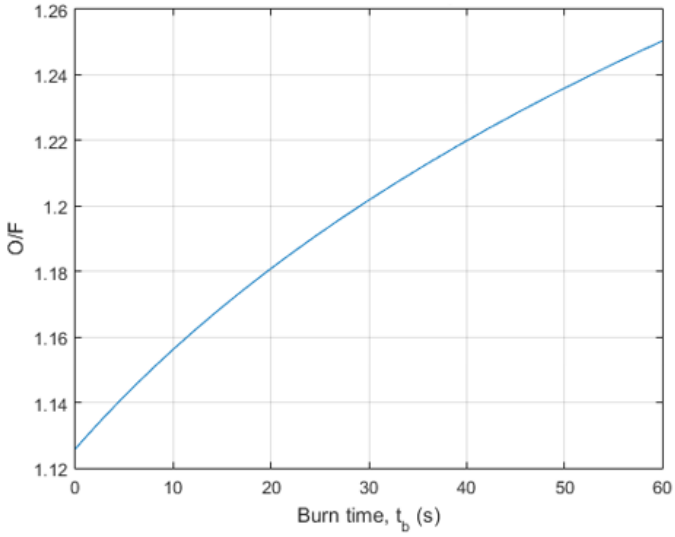

Figure 3. Variation of the mixture ratio throughout the burn interval.

3. REGRESSION RATE EQUATION ACQUISITION

According to Zilliac and Karabeyoglu (2006), the fuel regression rate is the receding rate of the fuel along the burn interval. Such parameter has a first order impact on the configuration and performance of a motor. In hybrid type motors, the average regression rate respects the relation presented by Eq. (1) (Cai *et al.*, 2011), where a is the regression constant, n is the flux exponent and $\overline{G}_{ox}$ is the average mass flux of oxidizer, which according to (Carmicino and Sorge, 2003) is expressed by Eq. (2), being the parameters $\dot{m}_{ox}$ and $\overline{D}$, the oxidizer mass flow rate and average port diameter, respectively.

$$\bar{\dot{r}} = a\bar{G}_{ox}^{n} \tag{1}$$

$$\overline{G}_{ox} = \frac{4\dot{m}_{ox}}{\pi\overline{D}^2} \tag{2}$$

The followed methodology to obtain the equations representing the regression rates is credited to DeLuca *et al.* (2011). The first step consisted of determining the ignition time (t_{ign}), established as the first instant at which the port appeared completely inflamed. All tests were recorded by a high-speed camera, and thousands of high-resolution images were available for analysis. An example of three frames captured at the instants of 0, 30 and 60 seconds of the same test is shown in Fig. 4, where the increasing port diameters over time can be observed.

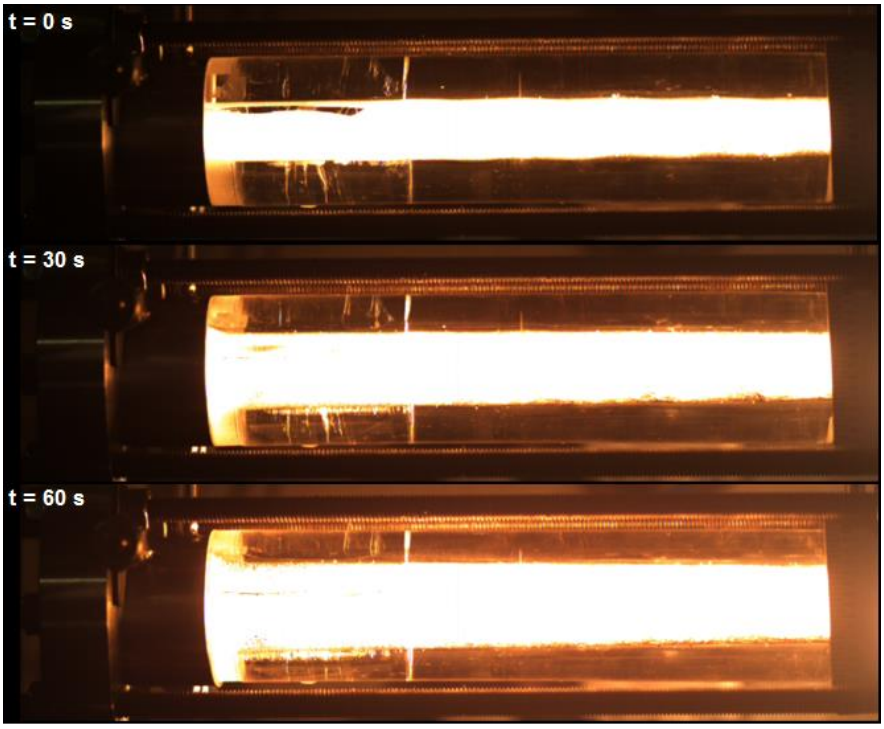

Figure 4. Images captured at 0, 30 and 60 seconds of the same test, illustrating the increasing port diameter over time.

The initial idea was to collect the average diameter from a set of images that had a five seconds interval between images. However, due to the expected low regression value for PMMA, to apply a visual data gathering method the appropriated interval showed to be a fifteen seconds interval. For every selected image the grain was divided in various cross sections, from twelve up to twenty depending upon the necessity to discretize the image to achieve higher quality results, and for each section the diameter was measured, resulting in an average diameter that captured even subtle variations. ImageJ (Rasband, 2016), a public domain processing program, provided a measuring tool used for the diameter measurements. Figure 5 is a generated screen by ImageJ that illustrates one selected frame that had the grain divided in twelve cross sections.

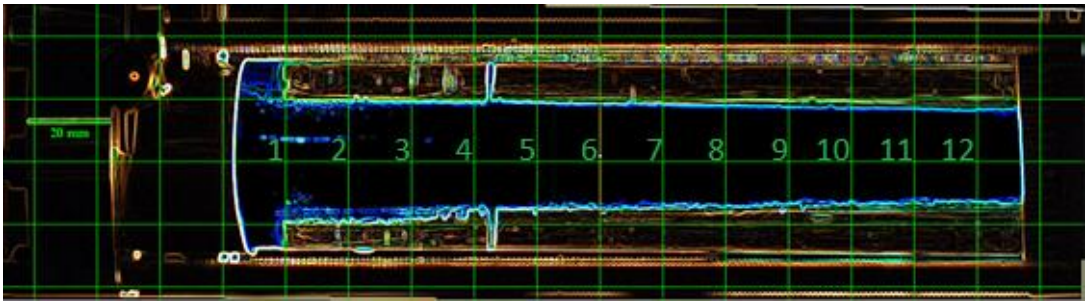

Figure 5. Illustration of a processed image used to determine the diameter variation along the grain's length.

Sequentially, a history of the port diameter in time could be achieved applying Eq. (4), where $\overline{D}(t)$ represents the instantaneous average port diameter, D_o is the initial diameter and the coefficients a_D and n_D were obtained through linear regression of $\ln(\Delta\overline{D})$ with respect to $\ln(t)$. In this case, i represents the number of the image and j, the section number.

$$\bar{D}_i = \frac{\sum_1^j D_{i,j}}{j} \tag{3}$$

$$\bar{D}(t) - D_o = a_D t^{n_D}, t \geq t_{ign} \tag{4}$$

After obtaining the coefficients a_D and n_D, it was possible to determine the average instantaneous regression rate through Eq. (5) and the oxidizer mass flux through Eq. (6).

$$\bar{r}(t) = \frac{1}{2} a_D n_D t^{n_D - 1}, \qquad t \geq t_{ign} \tag{5}$$

$$\bar{G}_{ox} = \frac{4\dot{m}_{ox}}{\pi(D_o + a_D t^{n_D})^2}, \qquad t \geq t_{ign} \tag{6}$$

A regression rate equation was finally obtained from the application of the Method of Least Squares for power curve fit (Thompson, 2010), with respect to the average instantaneous regression rate, $\bar{r}$ and the average oxidizer mass flux, $\bar{G}_{ox}$. The general format of a power curve is given by Eq. (7), in which the terms b and c are expressed by Eq. (8) and Eq. (9), respectively and N represents the amount of data.

$$y = cx^b \tag{7}$$

$$b = \frac{\sum ln\, x_i \, ln\, y_i - \frac{1}{N}(\sum ln\, x_i)(\sum ln\, y_i)}{(\sum (ln\, x_i)^2) - \frac{1}{N}(\sum ln\, x_i)^2} \tag{8}$$

$$c = exp\left[\frac{1}{N}\sum ln\, y_i - \frac{b}{N}\sum ln\, x_i\right] \tag{9}$$

An additional parameter associated to this method is the coefficient of determination, denoted by r^2, which is a statistical measure of how accurate the curve fitting is, regarding the experimental data. This parameter is expressed by Eq. (10).

$$r^2 = \frac{\left[\sum ln\, x_i \, ln\, y_i - \frac{1}{N}\sum ln\, x_i \sum ln\, y_i\right]^2}{\left[\sum (ln\, x_i)^2 - \frac{1}{N}(\sum ln\, x_i)^2\right]\left[\sum (ln\, y_i)^2 - \frac{1}{N}(\sum ln\, y_i)^2\right]} \tag{10}$$

Typically, when operating with opaque fuels such as paraffin for example, each test may provide only a single value for the oxidizer mass flux and regression rate, based on the initial and final characteristics of the fuel grain. However, choosing PMMA may be interesting from a didactic perspective due to the fact that more data can be acquired per experiment. It is possible due to the crystal characteristic of PMMA, which allows instantaneous visualization of the burn process.

4. EXPERIMENTAL SETUP

The designed, built and tested laboratory-scale hybrid rocket motor is shown in a schematic set-up in Fig. 6. The tests were conducted to acquire visual data to study and develop the regression rate equations associated to the burn of PMMA (fuel grain) and gaseous oxygen (GOX).

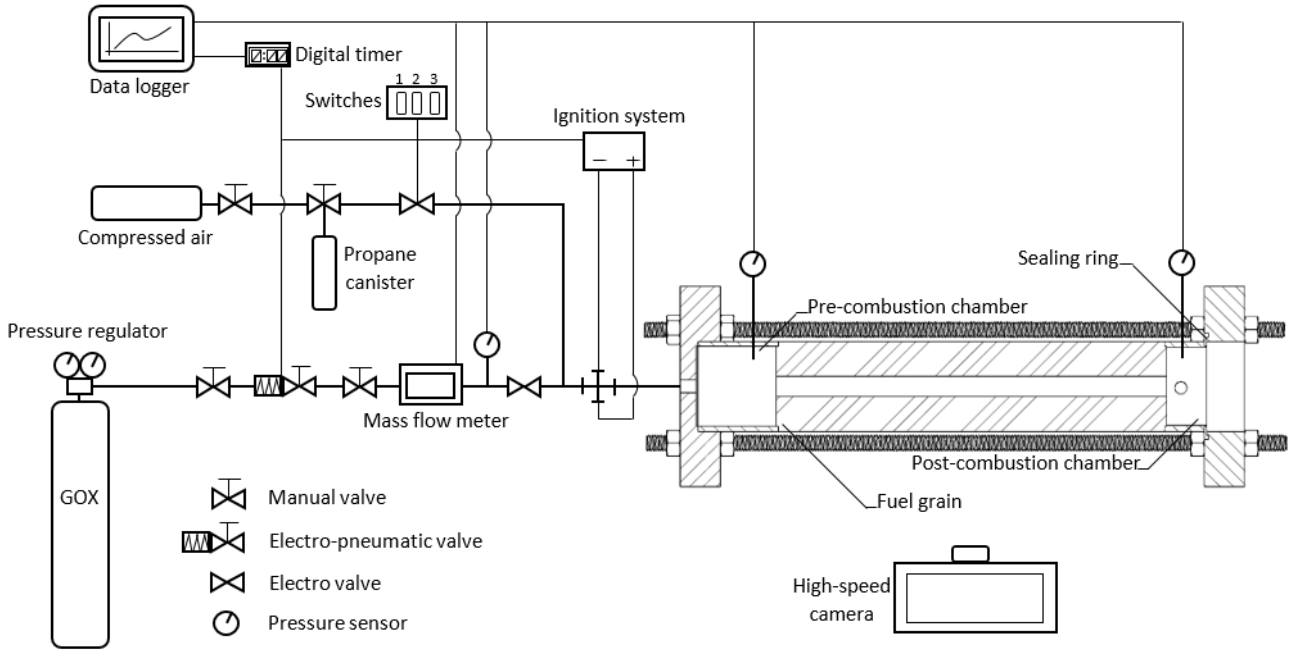

Figure 6. Schematic lab-scale hybrid rocket motor set-up.

The experiments were initiated by activating switch #1, which controlled the digital timer responsible for opening the electro-pneumatic valve and sending a signal to the data logger to start recording data from the pressure sensors and the mass flow meter. The activation of switch #2 supplied compressed air and propane to the experimental set-up, which in combination with oxygen provided a mixture for the ignition system. The activation of switch #3 produced a spark from the ignition system, then the mixture was deflagrated and a flame inside the grain was generated. The ignition system was composed of an inflammable gaseous mixture, and a spark generator, the same applied in regular stoves.

After the attachment of the flame to the grain, the supplies of propane and compressed air ceased and the oxygen flow was increased until achieving the oxidizer mass flow value specified by the design. The mass flow meter available for the measurements required a previous calibration for gaseous oxygen because it was originally for nitrous oxide.

From the moment that the flame attachment to the grain's inner surface was detected, the reaction occurred only due to the burn of PMMA and oxygen. All tests were recorded with a high-speed camera, positioned approximately fifty centimeters far from the fuel grain, for further analysis. The photograph in Figure 7 captures an instant of a completely inflamed combustion chamber during a test, and it is possible to see the high-speed camera gathering data.

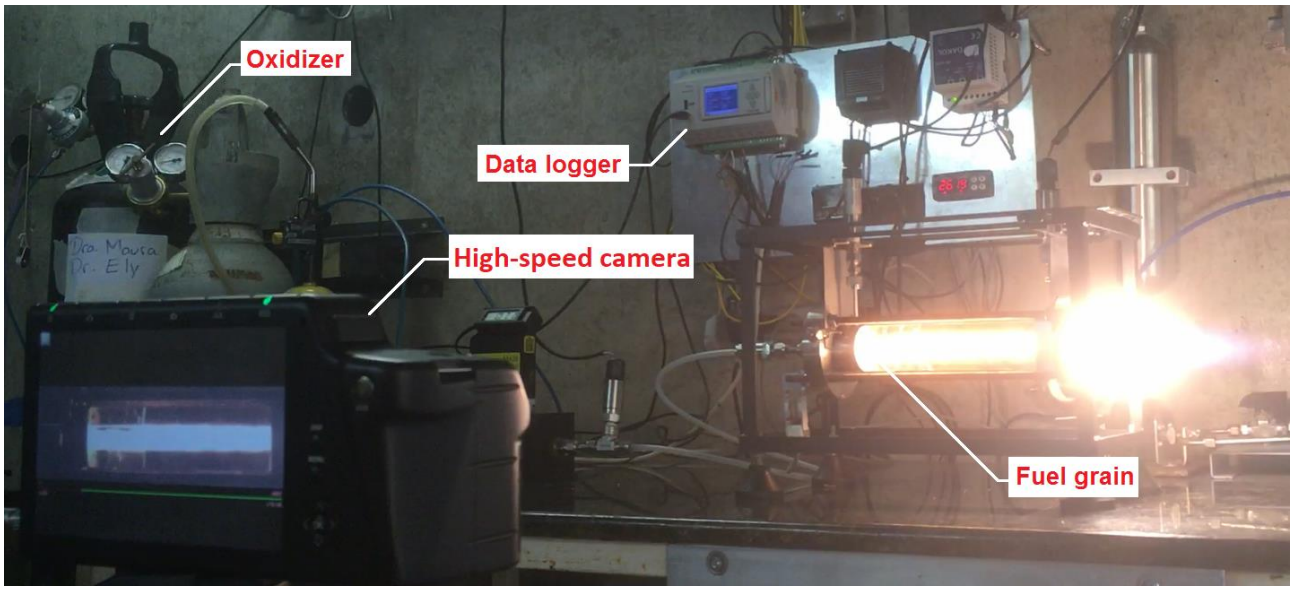

Figure 7. Representation of the experimental system during its operation.

5. RESULTS AND DISCUSSION

Throughout the testing phase, from the six tests carried out, twenty-three data points were obtained, what is considered a large amount of acquired data. Managing these data, it was possible to generate the curve fit representing the variation of the average regression rate with respect to the oxidizer mass flux, that resulted in $\bar{r} = 0.0499\bar{G}_{ox}^{0.5344}$, shown in Fig. 8.

In the Gox range of around 1 to 2 kg/m^{2}s, there are fifteen representative points from three tests that were operated with the apparatus at $\dot{m}_{ox} = 0.5\ g/s$, i.e. optimum conditions. Approximately at Gox of 0.3 kg/m^2s, three points were obtained from one test that ran with the mass flow rate below the optimum value. Above Gox of 2 kg/m^2s there is a total of five points that were obtained from two tests running each one with $\dot{m}_{ox} = 2\ g/s$ and $\dot{m}_{ox} = 3\ g/s$.

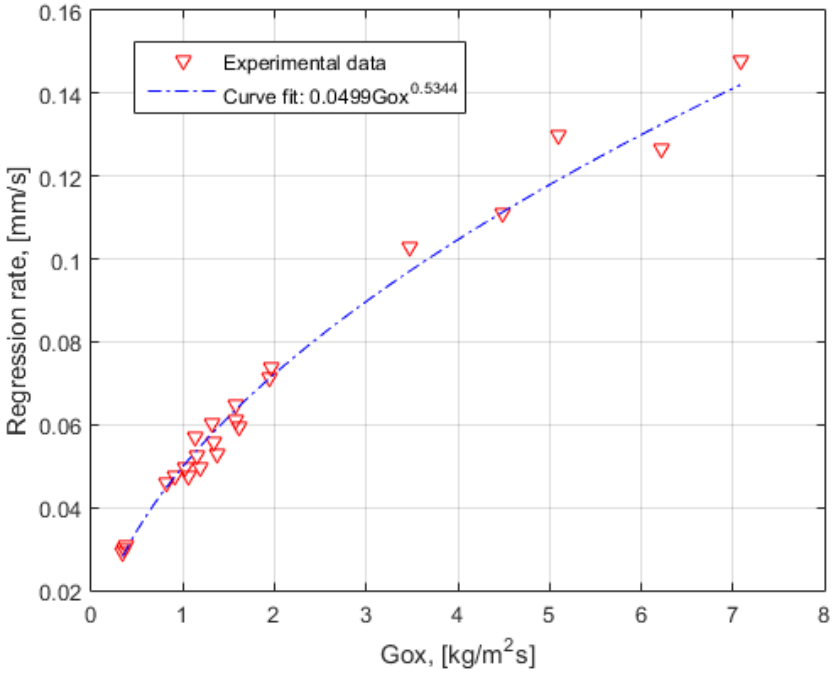

Figure 8. Regression rate expression acquired from the experimental data.

For comparison reasons Table 1 presents the regression rate equations obtained in the present research and from four other authors that worked with PMMA and oxygen as propellants. The five flux exponent values (n from Eq. 1) shown in Table 1 are in the range of 0.5 – 0.8 which is, according to Karabeyoglu *et al.* (2005), the most expected values for hybrid systems. It proves that the value of 0.5344 obtained in this work is in total accordance with the expectance. The curve fit produced the coefficient of determination (r^2) of 0.9849 that also validates the merit of the experimental data.

Table 1. Comparative data on the regression rate due to the burn of PMMA and oxygen.

	Fuel	**Oxidizer**	$\bar{G}_{ox}\ \left[\frac{kg}{m^2 s}\right]$	**Regression rate, [mm/s]**
Greiner and Frederick, (1992)	PMMA	O_2	7 - 700	$\bar{r} = 0.0219\bar{G}_{ox}^{0.6}$
Zilliac and Karabeyoglu, (2006)	PMMA	O_2	33 - 266	$\bar{r} = 0.0211\bar{G}_{ox}^{0.615}$
Pastrone, (2012)	PMMA	O_2	10 - 20	$\bar{r} = 0.0276\bar{G}_{ox}^{0.581}$
Cai *et al.*, (2013)	PMMA	O_2	4 - 1000	$\bar{r} = 0.0165\bar{G}_{ox}^{0.762}$
This work	PMMA	O_2	0.3 - 7	$\bar{r} = 0.0499\bar{G}_{ox}^{0.5344}$

6. CONCLUSIONS

Through the development of this work, the authors were able to design, build and operate a laboratory-scale hybrid system that allied simplicity and functionality in order to provide a feasible method to acquire and process data regarding one of the most important performance parameters when it concerns to rocket propulsion, the fuel regression rate. Due to the use of the experimental apparatus and to the choice of the PMMA as fuel for its crystal characteristic, it was possible to gather a large amount of data per experiment, which contributed to the achievement of a regression rate equation that was consistent with those found in the literature. Furthermore, facts such as the operational safety associated to hybrid propellants and low-cost of the propellants make this lab-scale hybrid device an attractive alternative for didactic applications.

7. REFERENCES

Cai, G., Zeng, P., Li, X., Tian, H. and Yu, N., 2013. "Scale Effect of Fuel Regression Rate in Hybrid Rocket Motor". *Aerospace Science and Technology,* Vol 24, p. 141-146.

Carmicino, C. and Sorge, A.R., 2003. "Investigation of the Fuel Regression Rate Dependence on Oxidizer Injection and Chamber Pressure in a Hybrid Rocket". In *Proceedings of the 39th AIAA/ASME/SAE/ASEE Joint Propulsion Conference and Exhibit.* Huntsville, Alabama.

DeLuca, L.T., Galfetti, L., Maggi, F., Colombo, G., Paravan, C., Reina, A., Tadini, P., Sossi, A. And Duranti, E., 2011 "An Optical Time-Resolved Technique of Solid Fuels Burning for Hybrid Rocket Propulsion". In *Proceeding of the 47th AIAA/ASME/SAE/ASEE Joint Propulsion Conference & Exhibit.* San Diego, California.

Frank, C., Durand, J.G., Evain, H. Tyl, C., Mechentel, F., Brunet, A. and Lizy-Destrez, S., 2014. "Preliminary Design of a New Hybrid and Technology Innovative Suborbital Vehicle for Space Tourism". In *Proceedings of the 19th AIAA International Space Planes and Hypersonic Systems and Technologies Conference.* Atlanta, Georgia.

Greiner, B. and Frederick, Jr. R.A., 1992. "Results of Labscale Hybrid Rocket Motor Investigation". In *Proceedings of the 28th AIAA/SAE/ASME/ASEE Joint Propulsion Conference and Exhibit.* Nashville, Tennessee.

Karabeyoglu, M.A., Cantwell, B.J. and Zilliac, G., 2005. "Development of Scalable Space-Time Averaged Regression Rate Expressions for Hybrid Rockets". In *Proceedings of the 41st AIAA/ASME/SAE/ASEE Joint Propulsion Conference & Exhibit.* Tucson, Arizona.

Kuo, K.K. and Chiaverini, M.J., 2007. *Fundamentals of Hybrid Rocket Combustion and Propulsion.* American Institute of Aeronautics and Astronautics, Inc. 1st edition.

Marxman, G., Gilbert, M., 1963. "Turbulent Boundary Layer Combustion in the Hybrid Rocket". *Symposium (International) on Combustion,* Vol. 9, p. 371-383.

Mathworks MATLAB, version R2009a: proprietary programming language. MathWorks, 2009.

McBride, B.J. and Gordon, S., 2002. "Chemical Equilibrium with Applications". 1 Aug. 2017 < https://www.grc.nasa.gov/www/CEAWeb/>.

Pastrone, D., 2012. "Approaches to Low Fuel Regression Rate in Hybrid Rocket Engines". *International Journal of Aerospace Engineering,* Vol. 2012, 12 pages.

Rasband, W.S., "ImageJ". U.S. National Institutes of Health, Bethesda, Maryland, USA, https://imagej.nih.gov/ij/, 1997-2016.

Sutton, G.P. and Biblarz, O., 2010. *Rocket Propulsion Elements.* John Wiley & Sons, New Jersey, 8th edition.

Thompson, D.E., 2010. "Curve Fitting – Method of Least Squares". 1 Aug. 2017 < https://www.engr.uidaho.edu/thompson/courses/ME330/lecture/least_squares.html >

Zilliac, G., Waxman, B.S., Dyer, J., Karabeyoglu, M.A. and Cantwell, B., 2012. "Peregrine Hybrid Rocket Motor Ground Test Results". In *Proceedings of the 48th AIAA/ASME/SAE/ASEE Joint Propulsion Conference & Exhibit.* Atlanta, Georgia.

Zilliac, G. and Karabeyoglu, M.A., 2006. "Hybrid Rocket Fuel Regression Rate Data and Modeling". In *Proceedings of the 42nd AIAA/ASME/SAE/ASEE Joint Propulsion Conference & Exhibit.* Sacramento, California.

8. RESPONSIBILITY NOTICE

The authors are the only responsible for the printed material included in this paper.